

From depth image to semantic scene synthesis through point cloud classification and labeling: Application to assistive systems

Chayma Zatout, Slimane Larabi

RIIMA Laboratory, USTHB University, 16111 Algiers, Algeria

USTHB University^a

^aBP 32 EL ALIA, 16111, Algiers, Algeria

Abstract

The aim of this work is to provide a semantic scene synthesis from depth image. First, depth image is segmented and each segment is classified in the context of assistive systems using a deep learning network. Second, inspired by the Braille system and the Japanese writing system Kanji, the obtained classes are coded with semantic labels. A semantic scene is then synthesized using the labels and extracted features. Experiments are conducted on noisy, occluded, cropped and incomplete data including acquired depth images of indoor scenes and datasets from the RMRC challenge. The obtained results are reported and discussed.

Keywords: Semantic labeling, Depth image, assistive systems, Point cloud classification, Deep learning, Scene synthesis

1. Introduction

In order to accomplish daily tasks, people involve their senses, namely sight, hearing, taste, smell and touch. Being deprived of one of the senses will complicate the process of accomplishing a given task; it will reduce human autonomy,

*Slimane Larabi

Email address: slarabi@usthb.dz (USTHB University)

URL: www.usthb.dz (USTHB University)

independence and even his privacy. Being deprived of the sight sense, visually impaired find difficulties in their daily life.

With the limitations of the classical aid systems such as white cans, guiding dogs and personal assistants; and with the evolution of technology, many commercial and noncommercial aid systems were proposed in the last decades. Generally, these latter rely on image processing, artificial intelligence techniques and external sensors in order to offer help for the visually impaired and blind people to improve their independence in many applications.

To transmit instructions, scene description or any other generated output, most of the assistive systems use audio-based or vibration-based output devices. It turns out that these latter hold hearing and are not too informative. Hence, the necessity of providing a semantic labeling for scene understanding that can be exploited by the touch sense which is often used to recognize people, obstacles, objects, and many other stuffs.

In this work, we propose an assistive system for the visually impaired and blind people based on two main modules: the classification module and the semantic labeling module. The first module is based on deep learning CNNs to classify depth image segments into seven semantic classes. The semantic labeling is inspired from Braille system and Kanji, a writing system. This latter is mapped into a touch-based synthesis area.

The remaining sections are structured as follows: in section 2, we present related works to objects classification, scenes understanding and semantic labeling for assistive systems. In sections 3, 4 we describe our approaches for the classification and semantic labeling . Conducted experiments are reported and discussed in section 5. Finally, we summarize the contributions made and we present planned future works.

2. Related Works

Visually impaired aid systems consist of set of techniques whose goal is to enhance the visually impaired life in different activities. These systems can

be traditional like white canes, guide dogs or personal assistants; sophisticated by involving advanced technologies and computer science or hybrid [1][2]. The sophisticated systems process the received data from real world using sensors and transform it into instructions and signs that can be understandable by the visually impaired people. They use depth or RGB sensors and techniques of image processing, computer vision and machine learning.

Many assistive aid systems have been proposed, in this work we focused on scene understanding and object detection, and semantic labeling.

2.1. Scene understanding and object recognition

Object recognition in complex scenes for general purpose is still a challenging problem. In recent work, Cupec *et al.* [37] recognize objects based on alignment of convex hulls of segments detected in a depth image with convex hulls of target 3D object models or their parts. This alignment is performed using the Convex Template Instance descriptor.

For visually impaired assistive systems, detecting objects is important in most applications. Knowing their nature will provides the ability to deduct additional information such as scene understanding, auto positioning and creating free space by moving some kinds of objects like chairs. In [3], they proposed a wearable system for recognizing and locating some types of obstacles using a depth camera. After detecting the ground, they used a linear classifier to classify the point cloud features into: chairs, tables, stair up, stair down and walls. The obtained class is coded and mapped into a braille display; so by touching the braille device, the user will understand what type of objects is in front of him. In [4], they proposed a system that uses Visual Odometry, Region-growing and Euclidean cluster extraction and depth data to determine if the horizontal planes are a valid step of a staircase. After the segmentation step, they transform the scene orientation into the Manhattan system; so the extracted planes can be classified into vertical or horizontal planes. In [5], scene understanding is achieved using deep learning techniques. The scene is captured using an RGB-D camera and the results are displayed using an earphone

and a smartphone that serves as a haptic device. They adapted FuseNet [6] and GoogleLeNe [7] to provide semantic segmentation and orientation instructions respectively. The semantic segmentation model was designed to predict 40 different classes; however, these latter are transmitted using an audio device.

In [8], point cloud is segmented based on cascaded decision tree using RGB-D images. They showed good results; however, the system only classifies a given segment, whether it is the ground, a wall or a table (a horizontal plane that is not the ground). As in [9], they proposed a lightweight CNN architecture that is able to be executed on smartphones for traveling assistive system. They adopted PeleeNet for object detection to cover 80 different classes using the RGB images as input.

2.2. Semantic labeling

In [10], they proposed a navigation system based RGB image processing. The system transmits the generated scene and the navigation instructions on the Senseg TM device. They used the electrostatic signs to generate codes and to form textural instructions for the visually impaired and blind people. They also used colors to encode additional visual feedback for the sighted and with low vision people.

In [3], they encoded the considered object classes using the first character of the class's name: o, c, t and a space to represent obstacles, chairs, tables and free spaces respectively. They used a braille device to transmit the occupancy grid to the user and to deliver object's label in the Braille system. These codes are simple to understand, but it can be ambiguous while covering a large set of objects, especially with objects having the same first character.

In our previous work [11], we proposed a semantic labeling for scene understanding since after understanding the scenes' components, a human-being can accomplish other tasks such as navigating. We mapped the detected planes into cylinders having a specific height and radius. These latter are mapped into a trapezoid area at a specific location. By touching this area, the user can locate objects from the free space that allows him to have an idea about their

characteristics, namely their heights and their areas.

Unfortunately, the proposed semantic labeling does not reveal the object's nature, it only gives an impression about the given object. For this reason, we propose in this work an improved semantic labeling that considers a set of important objects in indoors.

2.3. Discussion and Contributions

The discussed systems suffer from some limitations. In indoor navigation, for example, they do not provide a global description of the captured scenes; they usually consider only free space and consider the remaining components as obstacles without describing their nature. Knowing the nature of obstacles is important in many applications such as navigation. In other systems when objects are detected, they usually use an RGB camera as an additional input sensor. In [12], they classified objects into three classes: fixed objects, rearrangeable objects and transit objects. The fixed objects' class includes objects that are not rearrangeable, they are permanent and/or hard to uninstall such as stairs and elevators. The rearrangeable objects class includes objects that can be moved more or less easily. They can be small, medium such as tables and chairs; or larger such as dressers and refrigerators. As for the transit objects class, it represents self-moving objects or objects that are created by schedules. Thus, in the case of navigation, distinguishing between fixed and rearrangeable objects or even more precisely, differentiating between tables and chairs helps the visually impaired to create free paths by himself.

In other works, they provide obstacle classification, but by considering only few classes such as classifying the scene components into the floor, objects that are parallel to the floor and objects that are perpendicular to floor without considering other features such as the object's height and its occupied area. In case of object classification in visually impaired aid systems, the system's output is usually transmitted by an audio device. This latter suffers from some limitations as explained in [11] and in [13].

On the other hand, the current classification systems based on 3D data

are generally based on multi-view approaches when the data is gathered using a depth camera. In this case, having a clear multi-view of a given object is not convenient in many assistive applications. As an alternative, rotations are applied to the obtained object from a single frame [14], but this latter can be occluded, incomplete and cropped and thus applying several rotations around the yaw axis can be inconvenient too.

Regarding the semantic labeling, the current works are less informative and can generate ambiguity and do not considerate some geometric features that can be helpful. In [3] for example, the proposed semantic labeling that uses the first character of the class name, can become ambiguous when some classes start with the same character. The second character can be added, but it can generate ambiguity too.

Our main contributions in this paper are:

- A system based on deep learning networks to classify an object captured from a single frame with a depth camera. This classification is combined with our previous approach [11] in order to extend the number of possible classes and to provide additional information. Using only a depth camera as an input sensor reduces the computational complexity and the system's cost in terms of the required hardware.
- A semantic labeling that similar to the Braille and Kanji systems, can be mapped into a synthesis area. The proposed classification approach and its adequate semantic labeling will allow the user to have a clear idea about his surroundings and thus, he can perform several tasks alone.

Our proposed system (Fig. 1) takes a single depth frame captured by a head-mounted depth camera as an input. After detecting the ground using DCGD algorithm [11], the occupied space is extracted and segmented. Each computed segment is then fed to the deep network to perform object classification. Feature extraction module compute geometric features for each segment such as the object's height. After that, the provided class and features are used to generate

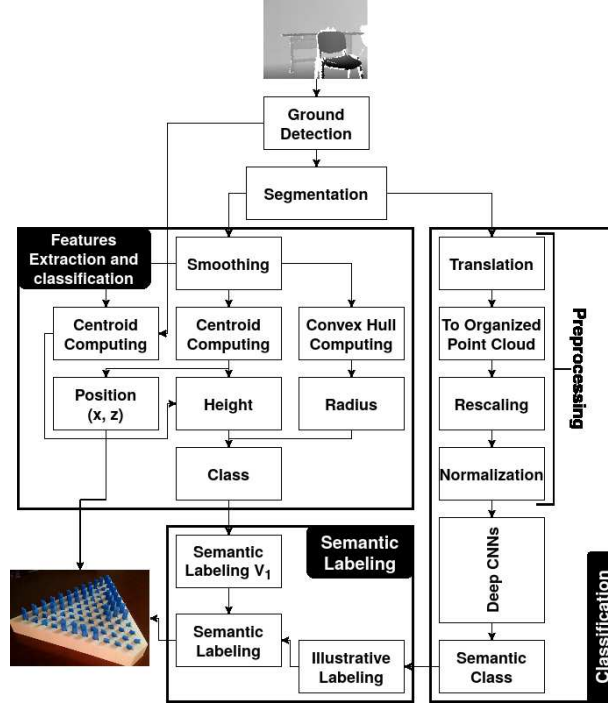


Figure 1: Our proposed framework, it consists of three essential modules. The ground detection module. The classification module that uses a deep model to predict the semantic classes. The feature extraction module that extracts geometric features. The output of these two modules are the input of the module that generate semantic labeling to be provided to a touch-based synthesis area.

semantic labels. Finally, a scene is synthesized based on the features and labels computed previously.

In the next section, we will present in details each system components, namely the classification module, the feature extraction module, the semantic labeling module, and the scene synthesis using coded objects that may serve as an output interface for assistive systems.

3. Point cloud Classification in the context of assistive systems

Our aim is to provide object classification in the context of assistive systems. In order to cover a significant number of classes in a simple way, we consider

salient objects (large and medium objects) and regroup them into 7 semantic classes that include 14 object classes, namely chairs, beds, sofas, benches, tables, desks, dressers, night-stands, shelves, bathtubs, toilets, windows, doors and stairs. These classes do not only contain semantic meaning, but the objects belonging to the same class have also a similar geometric shape while preserving some characteristics. The first class represents objects that we sit on, it includes chairs, beds, sofas and benches. The second class represents objects that we put something on, it includes tables and desks. The third class represents objects that we put, hide or arrange something in, it includes dressers, night-stands and shelves. As for the fourth, the fifth and sixth classes, they represent bathtubs and toilets; windows and doors respectively. The last class represents stairs and since the stairs can be dangerous for the visually impaired and blind people, making the difference between the stairs leading to upstairs and stairs leading to downstairs is important.

This module has two different modes: the off-line mode and the online mode. The first mode is when the training takes place. It is responsible for fixing the best CNN architecture and its weights to be used later. As for second mode, it represents when the system is running: after receiving a depth image, removing the ground and segmenting the point cloud into coarse segments, each segment is injected into the CNN model which was computed in the off-line mode.

3.1. Data preprocessing

After the segmentation step, instead of applying rotations, we translate the camera coordinates to a given pixel that is not zero. In this way, the obtained distances will be related to that pixel regardless of the camera’s position. Due to the noisy nature of the camera, we choose the center of mass of the image to avoid potential noises.

After that, we construct an organized point cloud from the depth image that contains only a single object after the segmentation step. An organized point cloud is a tensor $3 * w * h$ where 3 is the number of channels, w and h represents the width and the height of the bounding box after the scaling step. The first

channel, the second channel and the third channel hold the X values, the Y values and the Z values respectively. This step, can be skipped if the organized point cloud is already computed for 3D segmentation. It is skipped in the online mode since we used DBSCAN [38][39] for occupied space segmentation.

The scaling step is essential since the input’s shape of a given neural network is fixed and cannot be flexible for each entry. We used nearest neighbor interpolation in the scaling step. Feeding with the organized point cloud tensor will allow the neural network to learn the relation between the adjacent points on the three axes using convolutions. Finally, we apply data normalization in $[-1, 1]$ interval. We also investigated the use of normals instead of XYZ data.

3.2. Training

Deep learning architectures showed considerable improvement in many fields, especially with RGB data after introducing the Convolutional Neural Networks, CNNs. Current works investigate the 3D object classification using volumetric data [16][14][17] or point cloud [18][19][20][21] as input.

Since depth images are the input of our system, we investigated the behavior of different architectures used for image classification and selected the most accurate model. To do so, we trained the networks until they reach 100% as accuracy on training set or the training does not improve after some epochs. After that, we design a new architecture based on the selected neural network. The designed network has to be lightweight and accurate. Instead of starting training from scratch, we first took a pretrained model using data from the ImageNet challenge [22] and then, we investigated the fine-tuning technique before applying transfer learning. The fine-tuning approach has shown a weak performance since the nature of the inputs was different: the CNNs layers were initially trained from RGB images while we used XYZ data as input. For this reason, we opted for the transfer learning approach. The obtained results will be presented and discussed in section 5.

3.3. Features extraction and classification

In addition to the discussed object classification, we extract from the computed convex hull geometric features, namely object’s height and its occupied area as explained in [11]. This is done in the online mode, the offline mode is not needed for this classification. After the segmentation process, extracting geometric features and the classification is computed in parallel with the object classification.

This object description is useful for the visually impaired and blind people, it helps them to have an impression about their surroundings.

We combined these two classification methods, i.e. the classification using deep learning and the classification using the geometric features to provide rich information. For each object, we provide its semantic class, its height class and its occupied area class. When the deep learning model predicts the object class with low probability, only the second classification is maintained. In this way, we are sure to provide an accurate description even if the deep learning model fails to predict the right semantic class.

In addition, combining these classes allows the distinction between objects belonging to the same semantic class. Chairs, beds, sofas and benches are objects that we sit on; however, they are different in their forms and occupied area: beds are generally a large object (3rd class regarding the occupied area), chairs have small surface (1st class regarding the occupied area) and benches and sofas are medium objects (2nd class regarding the occupied area). Dressers, night-stands and shelves are all objects that we arrange something in; however, they have different heights and occupied areas: dressers are represented by the 3rd class regarding the height, night-stands are represented by the 2nd class, but shelves are usually medium objects and night-stands are usually small.

4. Object’s semantic labeling and scene synthesis

In this section, we introduce our proposed semantic labeling for indicating the class of each detected plane. Then, we describe how the perceived 3D scene

is synthesized into a specific area taking into account the located ground, the semantic label and extracted features of each 3D object.

4.1. Semantic labeling

In our previous work [11], we proposed our first semantic labeling: each horizontal plane in the scene was represented as cylinders with an associated height and radius that allow representing the occupied area and the height of the associated object respectively. This allows the user to have an impression about his surroundings: free space, small objects, medium objects, large objects and their heights, but it does not provide the object’s shape nor its nature: if it is a chair, a table, etc.

In this work, we propose an improved semantic labeling which takes into consideration the nature of the objects. It is inspired from the **Braille system** and **Kanji** (the Japanese writing system)(Fig. 2). An alphabet in Braille system is represented by a cell that is provided with raised dots. Each cell contains at most six raised dots. **Kanji** is a Japanese writing system that is inspired from logographic Chinese characters. Some Kanji letters that represent some objects are driven from nature, i.e. these objects’ shape in real-world; it’s the case for ‘mountain’ as shown in Figure 2 (right) first line.

In order to draw our illustrative semantic labeling, we designed cells with at most 25 raised dots. The cell’s shape can be revised depending on the precision of the synthesis area: if the synthesis area is rich in pins, we can design cells with more raised dots. We suggest to use cells such that the shape can be touched only by a single finger to avoid ambiguity.

On the other hand, the illustrative labeling is derived from the object’s shape in the real-world. For each semantic class, we chose the object that is the most close to the class’ meaning: we chose a chair, a table, a dresser, a bathtub, a window and a door to represent the proposed classes in section 3 respectively as shown in Figure 3. To ensure the user safety, we provide two different labels for the stairs leading to upstairs and stairs leading to downstairs as shown in Figure 4. In this way, by touch, the user will understand if he is about to climb

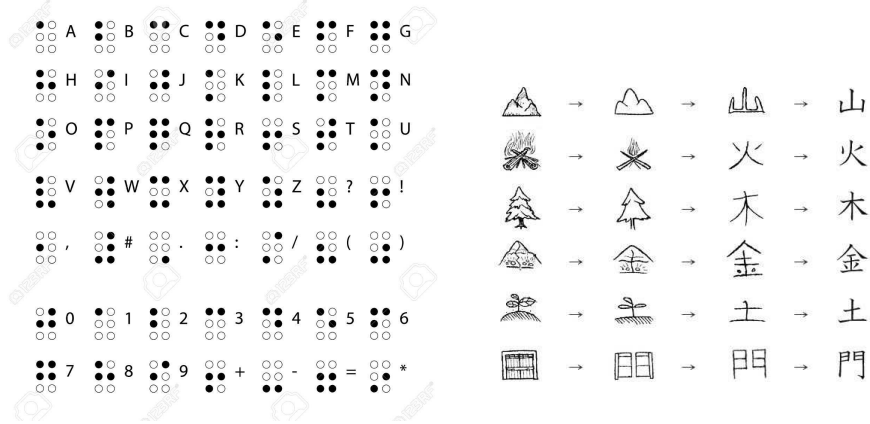


Figure 2: Left: the Braille system. Right: Kanji the Japanese writing system.

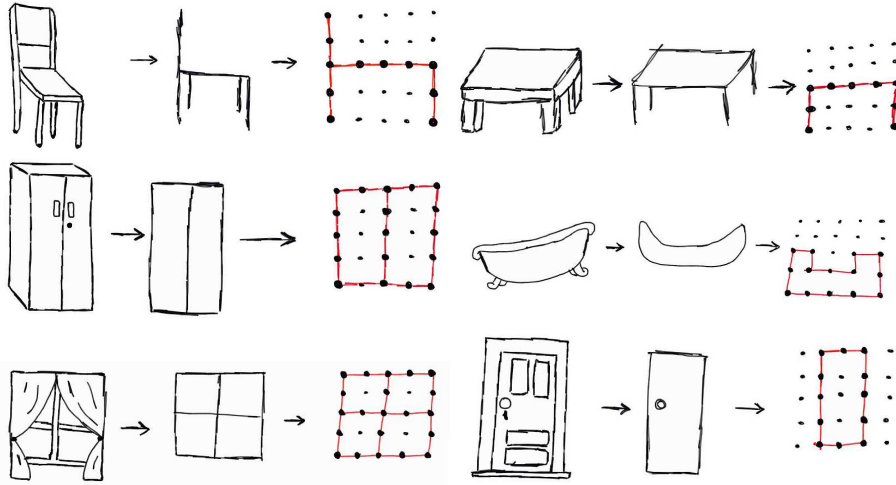


Figure 3: Our proposed semantic labeling from the first class to the last class, respectively (From top to down). We first drew the selected objects in the real-world (Left) and then, we derived shapes recursively until we obtained the current semantic labeling (From left to right).

the stairs or about to go downstairs.

The described labeling is used alongside with the first labeling to enrich the scene description. The reason we combined the two labels instead of creating an illustrative label for each object, is to reduce the number of possible illustrative

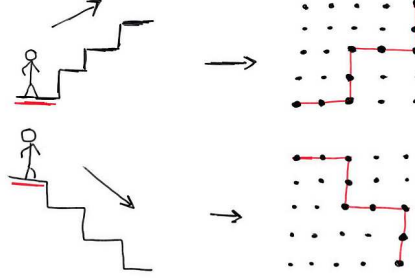


Figure 4: The proposed semantic labeling for stairs. Stairs leading to upstairs and leading to downstairs, their chosen labels, their positioning on the synthesis area.

labels since it can be deduced from its height and its occupied area.

4.2. Scene synthesis

The depth image acquired and processed gives as output: pixels of the ground and set of segments. To each segment is associated the class of the object, its label and extracted features.

The area of scene synthesis has a trapezoid shape corresponding to the scaled field of view of the camera. This area is composed by a dense number of pins that represents the raised dots in the Braille system. The pin may have **5** levels: The level zero is used to represent the holes on the ground. The level 1 represents the ground or the neutral element in some applications. The height of the illustrative labels, mapped in the center of the convex hull, is set to object's computed level (i.e. level 2, 3 or level 4) and the height of the remaining area of the convex hulls associated with the object is set to level 2.

The parameters of the depth camera are used to map the field of view into an the area of scene synthesis (see Fig. 5). Knowing that the ratio between the small and great basis of the trapezoid representing the field of view of the camera is equal to 5 (for $L = 400cm$), the scaled area of scene synthesis verifies the same ratio as indicated by figure 5)(right).

Let $b(x_b, y_b, z_b)$ be the barycenter of the box encompassing the object. The position of $b'(u_{b'}, v_{b'})$, the mapping of b on the synthesis area is calculated from

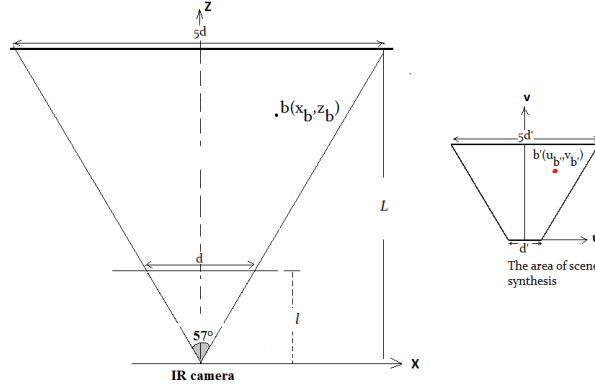


Figure 5: (Left) The field of view of the depth camera. (Right) The area of scene synthesis where semantic labels are generated.

the geometric relationship between the scene and the synthesis area as indicated by figure 5. The values of $u_{b'}$, $v_{b'}$ are given by the equations 1 and 2 where d' is the small basis of the synthesis area. The values of l , L for Kinect sensor are $80cm$ and $400cm$.

$$u_{b'} = d' \times x_b / d \quad (1)$$

$$v_{b'} = d' \times (z_b - l) / d \quad (2)$$

Let b_1, b_2, \dots, b_n be the points defining the box encompassing the object. In the same manner and using the equations 1, 2, the mapped points b'_1, b'_2, \dots, b'_n are located on the area. All pins inside the area defined by the points $b'_i, i = 1..n$ are set to level 2. The pins associated to the label of the object is set to their associated level 3, 4 or 5 at the barycenter as indicated by figure 6.

The area's input may receive the 3D raw data or labels. In figure 7, the point cloud of the captured scene is directly mapped on the area. The same point cloud is mapped into the synthesis area using different height of pins (see figure 8). For more visibility, we assigned the grey color, the green color, the red yellow color and the red color to represent objects with level 1, 2, 3 and 4 respectively.

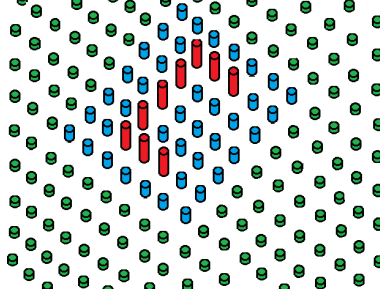


Figure 6: The convex hull and the positioning of the label (here for a table) on the area. Note that the pins of the label in red color are of level 3 (synonymous of the height of the table in the scene). The pins of the convex area in blue color are of level 2. The rest of the pins in the part of the synthesis area (in green color) are of level 1 correspond to the ground.

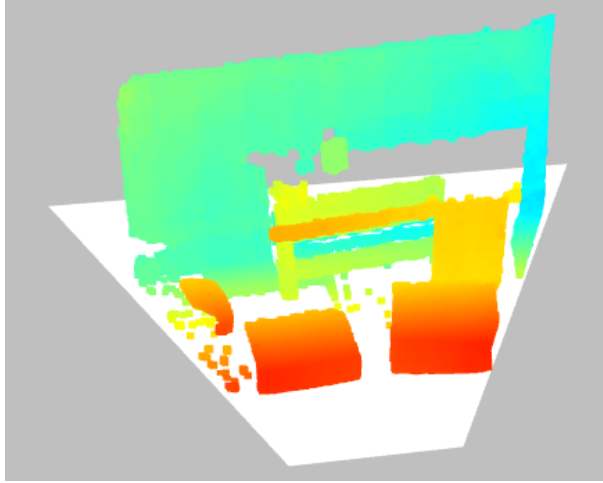


Figure 7: Mapping the 3D point cloud into the synthesis area.

5. Experiments

5.1. Experimental environment and used datasets

In order to perform the training, we ran our models on a GPU provided by the Google Colaboratory¹ platform. After that, we executed our proposed system on a laptop having i5 and 4GB as processor and RAM respectively.

¹<https://colab.research.google.com/>

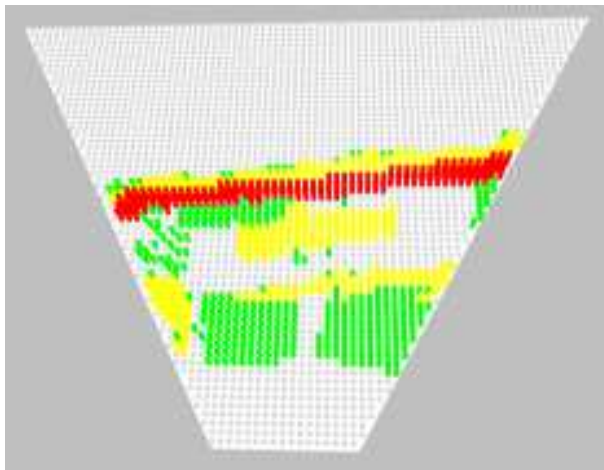


Figure 8: Scene synthesis from raw data (point cloud) using pins without semantic labeling.

Similar to [14] and [17], we used the data from the RMRC challenge². Since the dataset for 3D classification is no longer available in RMRC challenge (2014), we construct our data from its Semantic Segmentation Challenge. The data was initially consisted of 1800 RGB-D images with dense classification (23 possible classes). For each image, we considered only regions that belong to our selected classes (i.e. chairs, beds, sofas, benches, tables, desks, dressers, night-stands, shelves, bathtubs, toilets, windows, doors and stairs). The classes *windows*, *doors* and *stairs* were not among the 23 proposed classes so, in what follows we only consider the remaining classes. After the selection process, we obtained 3494 new images each of which represents one object only (a single segment). Table 1 represents the number of instances for each of the seven classes. We used the terms *chairs*, *tables* and *dressers* to represent the first three classes respectively. We also considered 35% of the data as the validation set. In addition, we used GDIS, our local dataset, for additional experiments. GDIS dataset was initially constructed for the ground detection task, but we considered some scenes for point cloud classification and the validation of the entire system (from

²<https://cs.nyu.edu/~silberman/rmrc2014/indoor.php>

the ground detection to the semantic labeling).

Table 1: The number of instances for each class.

Chairs	Tables	Dressers	Bath-tubs	Toilets
1595	934	786	80	99

5.2. Point cloud segmentation and feature extraction

In this work, we are interested in detecting and representing coarse information, i.e. large segments that represent salient objects. Detecting and transmitting coarse information in visually impaired assistive systems is important, knowing the scene architecture and how objects are arranged can be useful to accomplish many daily tasks such as scene understanding and navigation. Accordingly, in order to segment the obtained point cloud into coarse segments, clustering algorithms can be used for irregular object segmentation as mentioned in [25]. K-means [26] [27], mean-shift [28], fuzzy-clustering [29] and DBSCAN [30][31][32] clustering algorithms are widely used for point cloud segmentation. After testing K-means, min-shift and DBSCAN algorithms on a set of point clouds from our GDIS dataset (fig. 9), we selected the DBSCAN algorithm. It is suitable since our proposed system perform coarse segmentation. The DBSCAN is robust to noise, during clustering the noise is detected and classified as noise (fig. 9 third bottom image). In addition, it is a non-parametric algorithm, the number of clusters does not have to be defined beforehand unlike other clustering algorithms like K-means. To reduce the temporal complexity, we applied a downsampling on the input point cloud. A pass-through filter can be applied for noise removal; its parameters is fixed according to the characteristics of the depth camera. In our case, we only considered points with a depth between $800mm$ and $4000mm$ apart. After the segmentation step, each segment is injected into the classification module and the feature extraction and classification module.

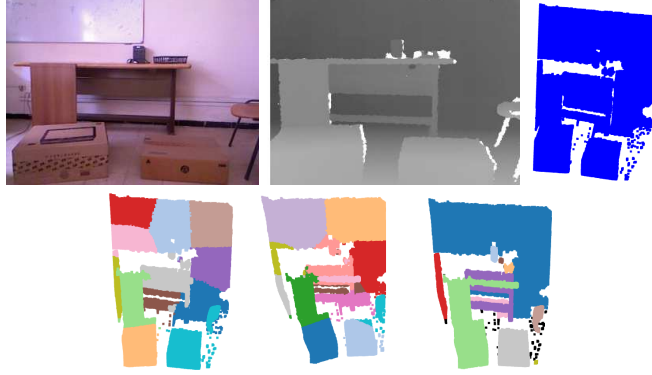


Figure 9: (Top) From left to right: color image, depth image and occupied space’s point cloud. (Bottom) From left to right: K-means, Mean-shift and DBSCAN. The DBSCAN detects noise (black points).

In this work, since we consider irregular segments and not planes, we computed the height differently compared to our previous work [11]. Instead of considering the difference between the ground’s and the centroid’s y – *coordinate*, we considered the height of the 90th percentile of the points’ y -coordinate. We chose the 90th percentile instead of the 100th to avoid potential outliers.

To evaluate this step, we took the measurements of some objects in the real-world and then compare it with the obtained geometric features. This is done by computing the Mean Absolute Error (MAE) between the objects’ measurements and the computed one. The obtained results showed a slight mean difference that does not exceed $30mm$.

5.3. Point cloud classification

5.3.1. Network selection

Several networks were proposed for object classification among which we cite: AlexNet [33], VGG16 [34], GoogleLeNet [7], ResNet [35] and MobileNet [36]. We took the pretrained model of each of the cited networks and we replaced the last dense layer with another dense layer for our classification purpose. We stop training if the accuracy does not progress after executing at least 30 epochs or if the model reaches 100% as training accuracy.

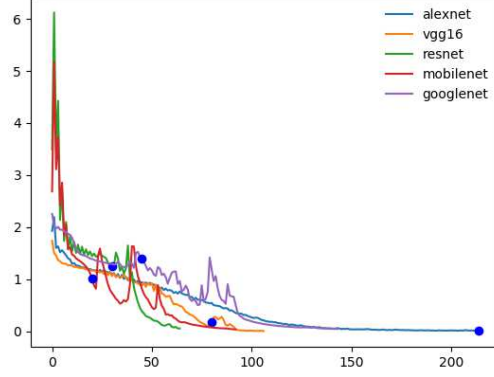


Figure 10: Comparison between the loss function of each tested model on training datasets. The blue marker represents the epoch where the model reached the highest accuracy on validation set.

Figures 10, 11 and Figures 12, 13 display the loss function and the accuracy on the training and the validation set respectively. Note that in this step, we did not apply any translations nor rotations. We wanted to study the architectures' performance without additional preprocessing.

The figures 10, 11, 12, 13 show an overfitting for all the models. In addition, the models' performance is not stable during training except for AlexNet model. This is due to the models' parameters, the nature of data, its complexity and the dataset size. The highest accuracy (the blue marker) on validation set is achieved at the same time as the highest accuracy on training set for only AlexNet model which showed smooth improvement during training; however, it was achieved while overfitting. The VGG-16 model achieved the highest accuracy (72.082%) on validation set.

5.3.2. Translation vs Rotation

As mentioned earlier, applying rotations on partially viewed objects is inconvenient. Hence, instead of augmenting data, rotations will sometimes act like a noise. In order to study their behavior, we trained the VGG-16 model

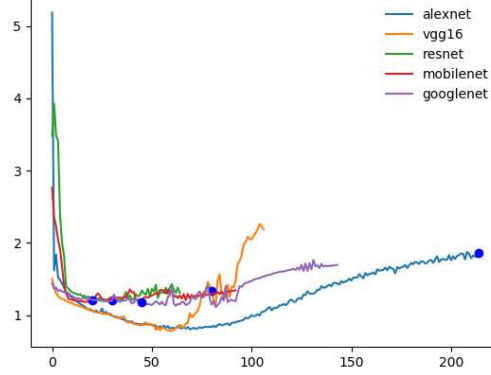


Figure 11: Comparison between the loss function of each tested model on validation datasets. The blue marker represents the epoch where the model reached the highest accuracy on validation set.

using translated and rotated point cloud separately (Fig. 14). We investigated both: offline augmentation and augmentation on the fly. The first method has shown a poor performance since the first iterations with an accuracy that does not exceed 3% on the test set. As for the second method, the over fitting has appeared after 61 epochs for the model with rotations while the model with translation has continued to improve for both: the training set and the test set.

5.3.3. Training

Based on the obtained results, we built our model based on VGG-16 by reducing the number of parts. We continued training after applying the presented data preprocessing. The model achieved an accuracy equal to 72,81% on the validation test (fig. 15) and 94.85% on our GDIS dataset (fig. 16 and fig. 17). Some layers have been removed from the VGG-16 architecture.

Figure 18 and Table 2 show the confusion matrix and the model's precision, recall and F-measure on each class respectively. The accuracy and the F-measure exceed 60% and 59% respectively for most classes. Although the

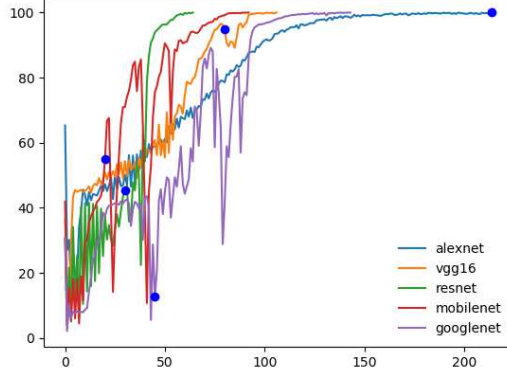


Figure 12: Comparison between the accuracy of each tested model on training datasets. The blue marker represents the epoch where the model reached the highest accuracy on validation set.

Table 2: The validation metrics of the CNN network on the test set.

	Bath-tubs	Chairs	Dressers	Tables	Toilets
Precision	0.545	0.778	0.669	0.630	0.667
Recall	0.214	0.823	0.691	0.586	0.647
F-measure	0.308	0.8	0.68	0.607	0.657

model’s accuracy on the class ‘*chair*’ is the highest, its F-measure is the lowest. This is due to the confusion between this class and the remaining classes (Fig. 18, column ‘*Chair*’). On the other hand, the class ‘*bath-tub*’ has low accuracy, but a high F-measure. This latter is due to the fact that the model mistakes the class ‘*bath-tub*’ for the other classes (Fig. 18, line ‘*Bath-tub*’), but it rarely mistakes the other classes for the class ‘*bath-tub*’ (Fig. 18, column ‘*Bath-tub*’). To visualize these latter, we display some samples from well classified instances and misclassified instances in Figure 19 and 20 respectively.

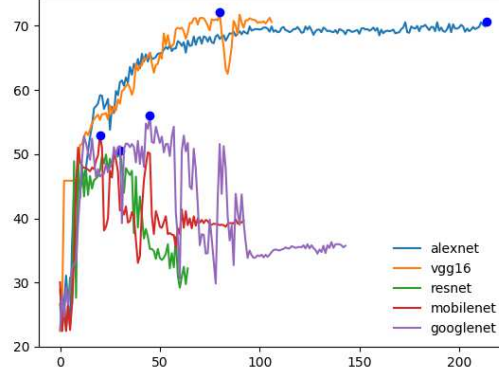


Figure 13: Comparison between the accuracy of each tested model on validation datasets. The blue marker represents the epoch where the model reached the highest accuracy on validation set.

5.4. Tests

For more experiments, we show and discuss the output of each module for 4 images taken from a video sequence from our GDIS dataset (fig. 21). After the ground detection (fig. 21 third row), we applied the DBSCAN clustering algorithm to break the occupied space into coarse segments (fig. 21 forth row). After that, we compute for each segment its geometric features and its class. The CNN network has classified well the chair except for the last frame (fig. 21 last row, last column), it was classified as a table with a low probability (0.6), so the class was not mapped, only the convex hull is mapped. The model failed to predict the right class because the chair’s point cloud was segmented into sub segments and this is due to the noisy nature of the Microsoft Kinect V1. If the class is not predicted, we set all the pins that represents the segment to the segment’s level, rather than mapping the class to that level.

5.5. Discussion

The proposed system combines the deep learning features and the geometric features to provide for the user a scene description: for each segment, its label,

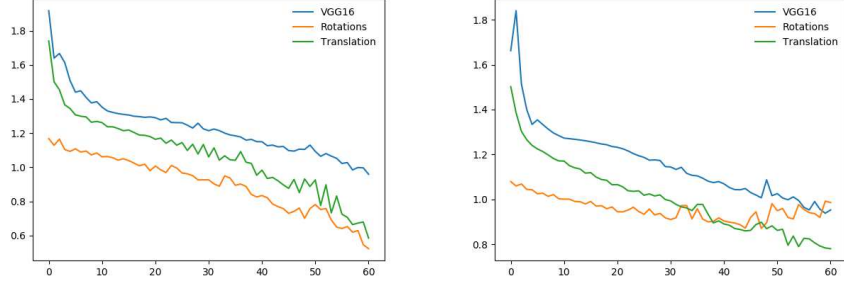


Figure 14: The loss function on training (left) and validation (right) data without and after applying rotations and translation.

location, shape, occupied space and its height are computed and mapped on the synthesis area.

Segmenting the point cloud is a crucial step, the accuracy of the computed features is highly dependent on it especially the geometric features. In this work, the DBSCAN algorithm is used since we were interested in coarse information. The DBSCAN is suitable in this case, since it is a clustering algorithm that is based on computing distance and density and without defining the number of clusters as initial parameter. In addition, it is robust to noise.

The system detects 7 semantic classes that cover 14 different object classes. For each semantic class, we proposed a semantic label which is mapped on the center of the occupied space. Providing and only mapping coarse information is the first step in the visually impaired assistive systems for the scene description task. It provides a global scene description of the captured scene and how the objects are arranged in. A second step can be added in the future for fine segmentation. In this step, objects that are arranged on a given coarse segment can be detected using coarse to fine segmentation. These latter, can be mapped on the synthesis area only by commands from the user to avoid ambiguity while exploring the scene. In other terms, mapping coarse and fine information at the same time is time consuming and ambiguous such as mapping the table and the objects that are on it. We can imagine this scenario: the user is searching for



Figure 15: Accuracy evolution by epochs on training and test sets. Although the model couldn't generalize well, the accuracy improves on both sets.



Figure 16: From left to right: the captured scene (chair, chair, chair), its associated depth image (the system input), the resulting segment, segment translation, the point cloud tensor as an RGB image. The system has predicted: chair, chair, chair.

a cup. After providing the global description, the user can locate the table on the synthesis area. After that, by long click on the table's label, we can at this time map on the whole surface of the area only the table and what's on it. At this step, by touching the new area's configuration, the user can have an idea

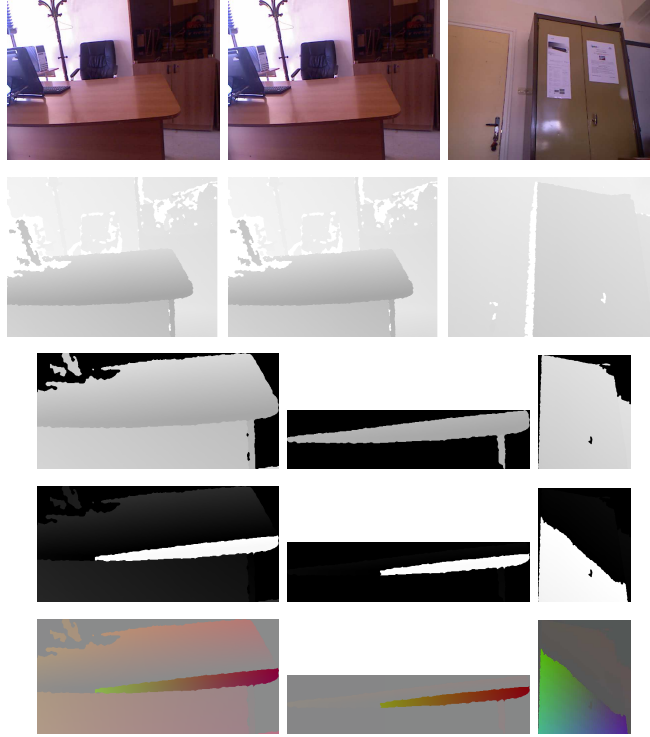


Figure 17: From top to down: the captured scene (table, table, dresser), its associated depth image (the system input), the resulting segment, segment translation, the point cloud tensor as an RGB image. The system has predicted: table, chair and dresser.

about what there are on the table and can search for his desired item.

The proposed system struggled for the following reasons: first, the training dataset was poor in terms of the number of instances and unbalanced: only 80 and 99 for the class 'Bath-tubs' and 'Toilets' respectively in contrast with the class 'chairs' (1595 instances). In addition, due to the nature of real-world data that is incomplete and cropped, false predictions can be occurred. Different cropped objects can be similar to some cropped objects belonging the different classes. Extending the used dataset by combining other datasets and/or by generating depth maps from CAD models can be a potential solution. After extending the dataset, we can apply transfer learning on the proposed model. We can also propose a new model which uses other types of data such as volumetric

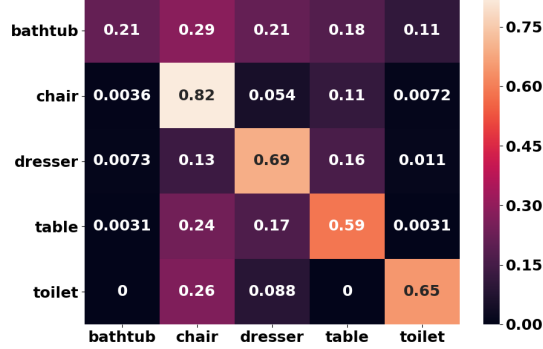


Figure 18: The confusion matrix of our selected model. The confusion matrix shows that there is some high confusion between objects having almost the same geometry: 26% of the toilet instances were confused with chairs and there is no confusion with tables and bathtubs.

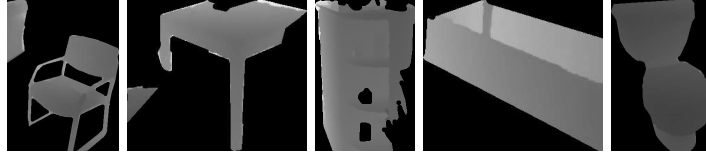


Figure 19: Sample from well classified instances. From left: Chair, Table, Dresser, Bath-tub and Toilet.

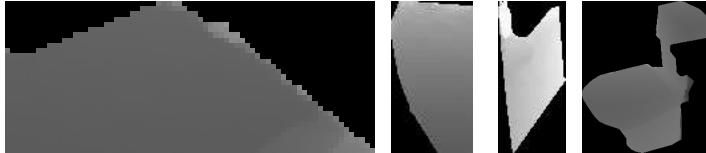


Figure 20: Sample from misclassified instances, the predicted class (class): Dresser (Chair), Chair (Table), Table (Bath-tub), Chair (Toilet)

data while reducing its computational and temporal complexity.

However, the achieved accuracy exceeded the accuracy obtained by the current 2.5D based models. Another advantage is the fact that the model ignores the predicted class if this latter has been predicted with a small probability. The model will map only the object’s convex hull and its height. The proposed model will be extended to work for a succession of frames and thus, the cropped

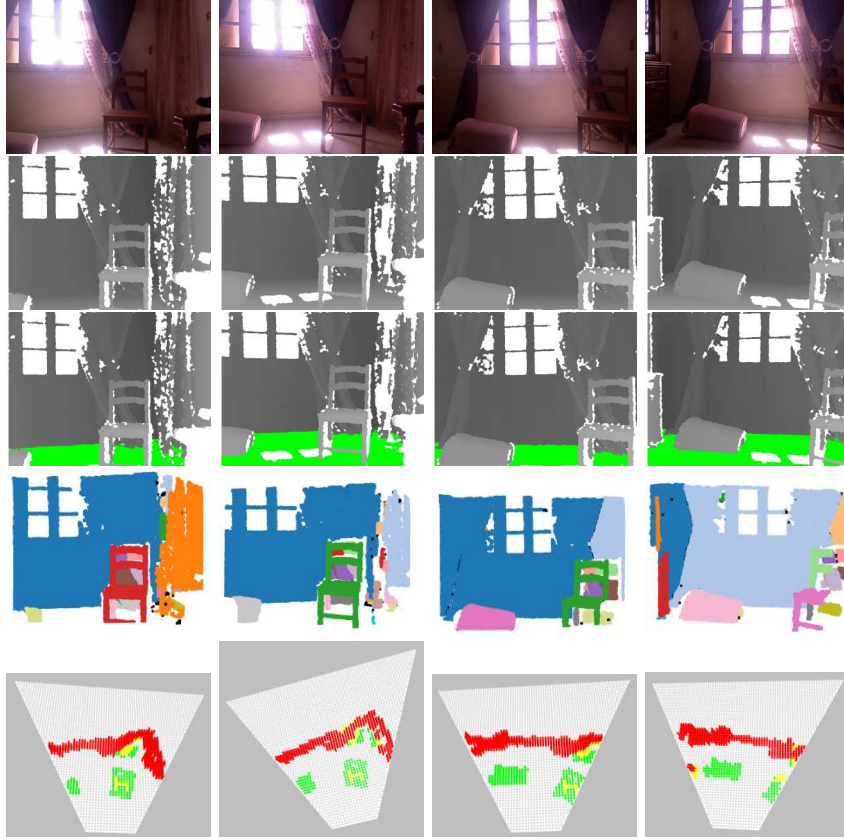


Figure 21: (From Top) The RGB image, the depth image, the output of the ground detection algorithm, the segmentation using DBSCAN and the semantic labeling mapped on the synthesis area.

objects can be completed by the alignment process and thus the prediction can be corrected.

6. Conclusion

In this paper, we proposed a framework for a semantic scene synthesis which can be used as an assistive system. It receives a depth image as the only input. After applying the segmentation, the system provides a class for each segment using our proposed classification method. Finally, it generates illustrative semantic labeling and map it into a synthesis area. The advantage of our system

is able to predict more than 15 classes only by understanding the provided illustrative labels (14 mentioned objects and the ground). For the remaining objects only their geometric features are transmitted.

In this work, we fixed the parameters such as the maximum height of an object that can be crossed, or the maximum size of a small object and a medium object as proposed in [11]. However, all the parameters can be adjusted after a clinical studies and tests. Another possibility is that these latter can be flexible for each user.

On the other hand, we aim to cover other object classes while enhancing the deep CNNs performance. We also aim to provide a detailed semantic labeling, in a clear way, to include not only salient objects like tables, but also other small objects.

Acknowledgments

This work has been supported by the Algerian grant for PhD studies PRFU number C00L07UN160420190001. The authors acknowledge the financial support of the Directorate General for Scientific Research and Technological Development (DGRSDT) of Algeria for the Research Laboratory in Intelligent Informatics, Mathematics and Applications (RIIMA).

References

- [1] M. Leo, G. Medioni, M. Trivedi, T. Kanade, G. Farinella, Computer vision for assistive technologies, *Computer Vision and Image Understanding* 154 (2017) 115.
- [2] T. R., B. Mocanu, T. Zaharia, Wearable assistive devices for visually impaired: A state of the art survey, *Pattern Recognition Letters*doi:<https://doi.org/10.1016/j.patrec.2018.10.031>.
- [3] H. Wang, R. K. Katschmann, S. Teng, B. Araki, L. Giarré, D. Rus, Enabling independent navigation for visually impaired people through a wear-

- able vision-based feedback system, in: 2017 IEEE international conference on robotics and automation (ICRA), IEEE, 2017, pp. 6533–6540.
- [4] A. Perez-Yus, D. Gutierrez-Gomez, G. Lopez-Nicolas, J. Guerrero, Stairs detection with odometry-aided traversal from a wearable rgb-d camera, *Computer Vision and Image Understanding* 154 (2017) 192205.
 - [5] Y. Lin, K. Wang, W. Yi, S. Lian, Deep learning based wearable assistive system for visually impaired people, in: *Proceedings of the IEEE International Conference on Computer Vision Workshops*, 2019.
 - [6] C. Hazirbas, L. Ma, C. Domokos, D. Cremers, Fusetnet: Incorporating depth into semantic segmentation via fusion-based cnn architecture, in: *Asian conference on computer vision*, Springer, 2016, pp. 213–228.
 - [7] C. Szegedy, W. Liu, Y. Jia, P. Sermanet, S. Reed, D. Anguelov, D. Erhan, V. Vanhoucke, A. Rabinovich, Going deeper with convolutions, in: *Proceedings of the IEEE conference on computer vision and pattern recognition*, 2015, pp. 1–9.
 - [8] Z. Wang, H. Liu, X. Wang, Y. Qian, Segment and label indoor scene based on rgb-d for the visually impaired, in: *International Conference on Multimedia Modeling*, Springer, 2014, pp. 449–460.
 - [9] J. Bai, Z. Liu, Y. Lin, Y. Li, S. Lian, D. Liu, Wearable travel aid for environment perception and navigation of visually impaired people, *Electronics* 8 (6) (2019) 697.
 - [10] J. Rivera-Rubio, K. Arulkumaran, H. Rishi, I. Alexiou, B. A.A., An assistive haptic interface for appearance-based indoor navigation, *Computer Vision and Image Understanding* 149 (2016) 126145.
 - [11] C. Zatout, S. Larabi, I. Mendili, S. A. E. Barnabé, Ego-semantic labeling of scene from depth image for visually impaired and blind people, in: *2019 IEEE/CVF International Conference on Computer Vision Workshops*,

- ICCV Workshops 2019, Seoul, Korea (South), October 27-28, 2019, IEEE, 2019, pp. 4376–4384.
- [12] W. Jeamwatthanachai, M. Wald, G. Wills, Map data representation for indoor navigation by blind people, *International Journal of Chaotic Computing* 4 (1) (2017) 70–78.
 - [13] J. Bai, S. Lian, Z. Liu, K. Wang, D. Liu, Smart guiding glasses for visually impaired people in indoor environment, *IEEE Transactions on Consumer Electronics* 63 (3) (2017) 258–266.
 - [14] D. Maturana, S. Scherer, Voxnet: A 3d convolutional neural network for real-time object recognition, in: *2015 IEEE/RSJ International Conference on Intelligent Robots and Systems (IROS)*, IEEE, 2015, pp. 922–928.
 - [15] C. Zatout, S. Larabi, A novel output device for visually impaired and blind people’s aid systems, in: *The First International Conference on Communications, Control Systems and Signal Processing*, 2020.
 - [16] S. Kumawat, S. Raman, Lp-3dcnn: Unveiling local phase in 3d convolutional neural networks, in: *Proceedings of the IEEE Conference on Computer Vision and Pattern Recognition*, 2019, pp. 4903–4912.
 - [17] Z. Wu, S. Song, A. Khosla, F. Yu, L. Zhang, X. Tang, J. Xiao, 3d shapenets: A deep representation for volumetric shapes, in: *Proceedings of the IEEE conference on computer vision and pattern recognition*, 2015, pp. 1912–1920.
 - [18] Y. Liu, B. Fan, S. Xiang, C. Pan, Relation-shape convolutional neural network for point cloud analysis, in: *Proceedings of the IEEE Conference on Computer Vision and Pattern Recognition*, 2019, pp. 8895–8904.
 - [19] J. Li, B. M. Chen, G. Hee Lee, So-net: Self-organizing network for point cloud analysis, in: *Proceedings of the IEEE conference on computer vision and pattern recognition*, 2018, pp. 9397–9406.

- [20] C. R. Qi, L. Yi, H. Su, L. J. Guibas, Pointnet++: Deep hierarchical feature learning on point sets in a metric space, in: Advances in neural information processing systems, 2017, pp. 5099–5108.
- [21] C. R. Qi, H. Su, K. Mo, L. J. Guibas, Pointnet: Deep learning on point sets for 3d classification and segmentation, in: Proceedings of the IEEE conference on computer vision and pattern recognition, 2017, pp. 652–660.
- [22] J. Deng, W. Dong, R. Socher, L. Li, K. Li, L. Fei-Fei, Imagenet: A large-scale hierarchical image database, in: 2009 IEEE conference on computer vision and pattern recognition, IEEE, 2009, pp. 248–255.
- [23] A. Zsaszimova, Alfabet braille ((accessed February 15, 2020)).
URL <https://se.dreamstime.com/alfabet-braille-engelsk-version-f>
- [24] J. Today, Why you must learn kanji (2012 (accessed February 15, 2020)).
URL <https://japantoday.com/category/features/opinions/why-you-must-learn-kanji>
- [25] Y. Xie, J. Tian, X. X. Zhu, A review of point cloud semantic segmentation, arXiv preprint arXiv:1908.08854.
- [26] R. Kuçak, E. Özdemir, S. Erol, The segmentation of point clouds with k-means and ann (artificial neural network), The International Archives of Photogrammetry, Remote Sensing and Spatial Information Sciences 42 (2017) 595.
- [27] S. Aparajithan, S. Jie, Clustering based planar roof extraction from lidar data, in: ASPRS 2006 Annual Conference, 2006.
- [28] T. Melzer, Non-parametric segmentation of als point clouds using mean shift, Journal of Applied Geodesy Jag 1 (3) (2007) 159–170.
- [29] J. M. Biosca, J. L. Lerma, Unsupervised robust planar segmentation of terrestrial laser scanner point clouds based on fuzzy clustering methods, ISPRS Journal of Photogrammetry and Remote Sensing 63 (1) (2008) 84–98.

- [30] T. Czerniawski, B. Sankaran, M. Nahangi, C. Haas, F. Leite, 6d dbscan-based segmentation of building point clouds for planar object classification, *Automation in Construction* 88 (2018) 44–58.
- [31] B. Wu, A. Wan, X. Yue, K. Keutzer, Squeezeseg: Convolutional neural nets with recurrent crf for real-time road-object segmentation from 3d lidar point cloud, in: *2018 IEEE International Conference on Robotics and Automation (ICRA)*, IEEE, 2018, pp. 1887–1893.
- [32] C. Wang, M. Ji, J. Wang, W. Wen, T. Li, Y. Sun, An improved dbscan method for lidar data segmentation with automatic eps estimation, *Sensors* 19 (1) (2019) 172.
- [33] A. Krizhevsky, One weird trick for parallelizing convolutional neural networks, *arXiv preprint arXiv:1404.5997*.
- [34] K. Simonyan, A. Zisserman, Very deep convolutional networks for large-scale image recognition, *arXiv preprint arXiv:1409.1556*.
- [35] K. He, X. Zhang, S. Ren, J. Sun, Deep residual learning for image recognition, in: *Proceedings of the IEEE conference on computer vision and pattern recognition*, 2016, pp. 770–778.
- [36] M. Sandler, A. Howard, M. Zhu, A. Zhmoginov, L.-C. Chen, Mobilenetv2: Inverted residuals and linear bottlenecks, in: *Proceedings of the IEEE conference on computer vision and pattern recognition*, 2018, pp. 4510–4520.
- [37] R. Cupec, I. Vidovic, D. Filko, P. Durovic. Object recognition based on convex hull alignment. *Pattern Recognition* 102 (2020), DOI: 107199.
- [38] M. Ester, H.P. Kriegel, J. Sander, X. Xu, et al., A density-based algorithm for discovering clusters in large spatial databases with noise., in: *Kdd*, Vol. 96, 1996, pp. 226-231.
- [39] E. Schubert, J. Sander, M. Ester, H. P. Kriegel, X. Xu, Dbscan revisited: why and how you should (still) use dbscan, *ACM Transactions on Database Systems (TODS)* 42(3), (2017) 1-21.